NASA / TM—1999-209275 AIAA–99–3510

Multiphysics Simulation of Active Hypersonic Cowl Lip Cooling

Matthew E. Melis
Glenn Research Center, Cleveland, Ohio

Wen-Ping Wang
Centric Engineering Systems, Sunnyvale, California

October 1999

The NASA STI Program Office . . . in Profile

Since its founding, NASA has been dedicated to the advancement of aeronautics and space science. The NASA Scientific and Technical Information (STI) Program Office plays a key part in helping NASA maintain this important role.

The NASA STI Program Office is operated by Langley Research Center, the Lead Center for NASA's scientific and technical information. The NASA STI Program Office provides access to the NASA STI Database, the largest collection of aeronautical and space science STI in the world. The Program Office is also NASA's institutional mechanism for disseminating the results of its research and development activities. These results are published by NASA in the NASA STI Report Series, which includes the following report types:

- TECHNICAL PUBLICATION. Reports of completed research or a major significant phase of research that present the results of NASA programs and include extensive data or theoretical analysis. Includes compilations of significant scientific and technical data and information deemed to be of continuing reference value. NASA's counterpart of peer-reviewed formal professional papers but has less stringent limitations on manuscript length and extent of graphic presentations.

- TECHNICAL MEMORANDUM. Scientific and technical findings that are preliminary or of specialized interest, e.g., quick release reports, working papers, and bibliographies that contain minimal annotation. Does not contain extensive analysis.

- CONTRACTOR REPORT. Scientific and technical findings by NASA-sponsored contractors and grantees.

- CONFERENCE PUBLICATION. Collected papers from scientific and technical conferences, symposia, seminars, or other meetings sponsored or cosponsored by NASA.

- SPECIAL PUBLICATION. Scientific, technical, or historical information from NASA programs, projects, and missions, often concerned with subjects having substantial public interest.

- TECHNICAL TRANSLATION. English-language translations of foreign scientific and technical material pertinent to NASA's mission.

Specialized services that complement the STI Program Office's diverse offerings include creating custom thesauri, building customized data bases, organizing and publishing research results . . . even providing videos.

For more information about the NASA STI Program Office, see the following:

- Access the NASA STI Program Home Page at ***http://www.sti.nasa.gov***

- E-mail your question via the Internet to help@sti.nasa.gov

- Fax your question to the NASA Access Help Desk at (301) 621-0134

- Telephone the NASA Access Help Desk at (301) 621-0390

- Write to:
  NASA Access Help Desk
  NASA Center for AeroSpace Information
  7121 Standard Drive
  Hanover, MD 21076

NASA / TM—1999-209275 AIAA–99–3510

Multiphysics Simulation of Active Hypersonic Cowl Lip Cooling

Matthew E. Melis
Glenn Research Center, Cleveland, Ohio

Wen-Ping Wang
Centric Engineering Systems, Sunnyvale, California

Prepared for the
1999 Norfolk Summer Conference
sponsored by the American Institute of Aeronautics and Astronautics
Norfolk, Virginia, June 28—July 1, 1999

National Aeronautics and
Space Administration

Glenn Research Center

October 1999

Acknowledgments

Special thanks are due to Drs. Bob Ferencz and Steve Rifai for helpful discussions during the course of this study.

Available from

NASA Center for Aerospace Information
7121 Standard Drive
Hanover, MD 21076
Price Code: A03

National Technical Information Service
5285 Port Royal Road
Springfield, VA 22100
Price Code: A03

MULTIPHYSICS SIMULATION OF ACTIVE HYPERSONIC COWL LIP COOLING

Matthew E. Melis
National Aeronautics and Space Administration
Glenn Research Center
Cleveland, OH 44135

and

Wen-Ping Wang
Centric Engineering Systems
Sunnyvale, CA

Abstract

This article describes the application of the Multi-disciplinary Analysis (MDA) solver, Spectrum ™, in analyzing a hydrogen-cooled hypersonic cowl leading-edge structure. Spectrum, a multi-physics simulation code based on the finite element method, addresses compressible and incompressible fluid flow, structural, and thermal modeling, as well as the interactions between these disciplines.

Fluid-solid-thermal interactions in a hydrogen impingement-cooled leading edge are predicted using Spectrum. Two- and semi-three-dimensional models are considered for a leading edge impingement cooling concept under either specified external heat flux or aerothermodynamic heating from a Mach 5 external flow interaction. The solution accuracy is demonstrated from mesh refinement analysis. With active cooling, the leading edge surface temperature is drastically reduced from 1807 K of the adiabatic condition to 418 K. The internal coolant temperature profile exhibits a sharp gradient near channel/solid interface. Results from two different cooling channel configurations are also presented to illustrate the different behavior of alternative active cooling schemes.

Introduction

Necessary to advancing the state-of-the-art of technologies for hypersonic flight vehicles is the development of an airframe and propulsion system capable of withstanding sustained high thermal, aerodynamic, and structural loads expected during flight. In these systems, the engine cowl leading edges are anticipated to have some of the most severe exposure to these loads and hence, are considered to be a critical system for enabling the development of a hypersonic aircraft. To prevent material failure on the cowl lip caused by high aerodynamic heating, including effects of stagnation and shock-on-shock interactions, active cooling schemes for the leading edges may be desirable. It is expected that these systems would likely be cooled by cryogenic hydrogen carried as a fuel on board the aircraft.

Many actively cooled leading-edge concepts have been proposed in recent years to address this technology challenge. Design of such a structure is difficult when incorporating all of the loads, and their respective interactions, as it involves analyses in three separate and highly complex disciplines: Fluid Dynamics, Heat Transfer, and Structural Mechanics. Typically, these analyses would be performed independently and the results would be passed between analysts in a piecemeal fashion. Each of the analysis results affects the other two and thereby mandates an iterative process to reach a converged solution. The process ultimately results in a very cumbersome and inefficient task. In many cases, it would be more efficient to use a simplified method to design and test several variants of a component as opposed to trying to arrive at a design through computational analyses. Recent advances in multiphysics analysis techniques, however, have made this latter choice more attractive. Centric Engineering Systems has developed Spectrum™, a finite-element based analysis package which can simultaneously solve fluid (incompressible and compressible), thermal, and structural interactions for a wide class of problems using a single-pass solution approach.

The thermal-solid analyses have been performed by Melis et al. [1] to demonstrate the feasibility of several design concepts for leading edge cooling. Different internal cooling configurations including

cross-flow, parallel and impingement were considered with limited experimental data to support the research. The cooling effectiveness of the various concepts was demonstrated by finite element analysis; however, the analyses were limited by the use of empirical formulations for both the external and internal fluid dynamics.

The purpose of this paper is to demonstrate Spectrums ability to perform a single pass fluid-thermal-structural analysis of an impingement hydrogen-cooled leading-edge concept made of nickel in a Mach 5 flight condition. The results of fluid (incompressible and compressible)-solid-thermal (FSI) interactions between internal hydrogen coolant, the structure, and the external hypersonic flow will be presented. Both two-dimensional and semi three-dimensional (3D structure, 2D fluid) models will be considered. Mesh refinement results will also be discussed to validate solution convergence.

Methods

Spectrum's multiphysics architecture supports multiple physical interactions through a data model defined as a hierarchical tree of regions and interfaces. Regions of a problem are used to separate the different physics being analyzed over the spatial domain. For example, in a fluid-structure interaction problem, the fluid domain is one region and the solid structure is another (Figure 1). Within each region, sub-regions are allowed for different element technology and material modeling. Interfaces are used to enforce the coupling constraints between the different regions. A slave-master algorithm is then used to define the discrete interface constraints of multi-physics problems. These constraints are enforced with the augmented Lagrangian formulation. The technologies underlying the finite element methods used in the Solver are described in References [2]-[8] and [20].

The finite element treatment of fluid regions within this framework is based on the Galerkin-Least-Squares (GLS) method with discontinuity capturing operators. In this treatment, the compressible flow formulation makes use of *physical entropy variables.* With these variables, the fluid conservation laws are expressed in symmetric form, which intrinsically expresses the mathematical and physical stability provided by the second law of thermodynamics. In turn, the finite element techniques employed herein inherit this fundamental stability, and some limited convergence proofs are available. Since entropy variables do not yield the most efficient form of the incompressible equations with the absence of shocks and discontinuities, the state variables are hence used in the incompressible flow formulation.

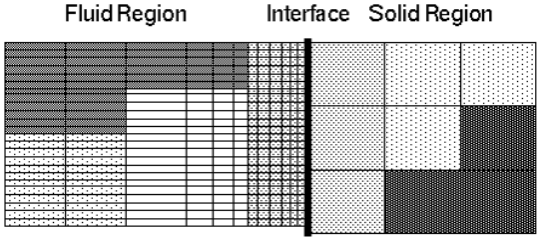

Figure 1. Problems are divided into regions to analyze multiple disciplines. Interfaces between regions are defined on surfaces with varying mesh discretizations.

Multiphysics problems often require the movement of the computational fluid domain in response to the deformation of the common solid region boundaries. The arbitrary-Lagrangian-Eulerian (ALE) method is utilized to account for the deformations in fluid domains ([9], [10]).

Within solid regions, the finite element treatment of structures is based on the Hu-Washizu variational principle, e.g., [11]. These methods are well documented in the literature to address numerical locking phenomena. The kinematic description admits small and finite deformations and strains. The structural formulations (beams and shells, [12]) are expressed in resultant form. The exponential map is employed for rotational updates, which are geometrically exact, and singularity free. Linear and nonlinear material models are used for the constitutive relations with thermo-mechanical coupling. The structural elements are coupled to all of the material models in the constitutive library.

Spectrum has been applied to numerous multi-physics problems. Selected applications are demonstrated in References [13]-[17]. In particular, in Reference [15], an Interior Comfort Engineering (ICE) system was developed to allow the design of automotive climate control systems, and Spectrum was used as the simulation engine to predict the thermal load. It was found that under a solar soak transient simulation the ICE system was able to attain an accuracy level of approximately 4.0 C (with the averaged interior temperature of 60.0 C) as compared to the wind tunnel data.

Computational Problem Description

An impingement cooled leading-edge configuration was modeled loosely around the hypersonic strut leading edge detailed in Reference [18]. This concept consists of a series of channels in the center of the structure, which bring coolant to impinge directly onto the leading edge tip. The cooling flow then splits and is directed back through channels to cool the top and bottom surfaces of the leading edge structure. Figure 2 illustrates a cooling channel for the impingement scheme with the pertinent physical dimensions highlighted.

To utilize symmetric conditions, only a section of the test piece with a single coolant duct is simulated here. As mentioned earlier, we will limit our investigation in this paper to two-dimensional and semi-three-dimensional flow calculations. To develop confidence in the solution accuracy, a 2D model of thermal coolant and solid model interactions under a specified external heat flux was performed first (hereafter Case 1). Next full 2D interactions of hydrogen coolant, nickel solid, and external hypersonic flow was simulated (Case 2). Finally, two semi-3D models (incorporating a full 3D structures model with 2D flow models) with different channel configurations were studied to determine effectiveness of the active cooling concepts (Case 3).

This impingement concept has been tested in a hot gas facility to assess its effectiveness [1]. But the extreme environments have severely hampered efforts to obtain accurate steady state temperature data from the test piece and thus making direct comparison with current simulations impossible. Nevertheless, coolant inlet conditions were used from these experiments as a baseline for the analyses to match closely with the experiment condition. The ambient temperature is taken at 278 K, the coolant inlet duct velocity is specified at 278 m/sec, and the hydrogen density is 3.573 Kg/m^3. The rest of hydrogen properties are taken from standard conditions listed in Reference [19]. The resulting Mach number is about 0.2 and Reynolds number is about 1.0E5. As a result, the coolant flow is considered incompressible and the Spalart-Allmaras turbulence model is employed to model the expected turbulent physics. Standard properties (listed in [19]) are also employed for the nickel solid model whereas a temperature dependent thermal conductivity is adopted.

The external compressible air has an inlet temperature of 300 K and Mach number of 5. Although the flow regime falls into the lower end of the hypersonic range, a perfect gas assumption is still considered adequate for the present purpose. Since the internal hydrogen coolant is considered incompressible, the thermal equation is essentially decoupled from the fluid equations. However, in external flow, the thermal variable is coupled directly with the fluid variables. In essence, a multiphysics conjugate heat transfer problem between the coolant, the nickel solid and the external hypersonic flow is simulated.

The Spectrum solver supports different degrees of coupling via the stagger and solution strategy [20]. In the present study, a segregated approach is employed for the coolant calculation consisting of pressure, velocity, and turbulence staggers. Another stagger for the thermal stress equation is employed. The compressible flow equations, along with the solid and coolant thermal equations, make up the final stagger. The steady state solution is achieved when the overall stagger iteration converges.

Figure 3 depicts the mesh (i.e., mesh 2) used in Case 1 and 2. For clarity, the mesh in all three regions (coolant channel, solid model and external flow) is shown here in both global and local views near the leading edge. A total of 27,154 nodes and 12,905 8-node hexahedral elements were used. The internal coolant mesh has been refined near the wall to capture the turbulent and thermal boundary layers. The external flow mesh has also been refined near the wall to capture the boundary layers. It should be noted that both the fluid and solid mesh consist of three-dimensional elements (with one element through the thickness); however, the flow was computed as two-dimensional as Spectrum handles 2D computations using this element type.

Results

Case 1: 2D coolant and solid thermal interactions

This case predicts the thermal interactions under a specified heat flux on the solid surface. The heat flux distribution has a maximum of 1.3E7 W/m^2 at the nose tip and then tapers off to 1.25E6 exponentially downstream to simulate aerothermodynamic heating.

The steady-state coolant flow fields for the pressure contours, total velocity magnitude contours, and velocity vectors are depicted in figures 4-6. Figure 4 illustrates the pressure contours in both

global and local views. It is seen that the pressure reaches a maximum near the nose region indicating flow stagnation. In Figures 5 and 6, the flow, as expected, impinges upon the solid leading edge and turns and splits in the opposite direction along the outer skin of the test model. Additionally, small circulation pockets are clearly present at the edge of the internal duct as evidenced by the low pressure and high velocity contours.

The steady-state temperature contours for the internal coolant and the solid models are shown in figures 7-9. Figure 7 illustrates the thermal contours in global view. The spatial-varying external heat flux prescribed results in a high temperature concentration near the nose and then levels off downstream. The maximum temperature at the nose is 825 K (legend shown in figure 8). Note that Killackey et. al. have predicted a peak temperature of 1016 K under maximum heat flux 1.8 W/m^2 at the tip.

The thermal gradient in the solid region as expected is nearly linear (weak nonlinearity coming from temperature-dependent thermal conductivity) as can be seen in figure 8. In contrast, a steep temperature gradient is found inside the coolant region. (In the coolant stagnation region, the thermal boundary layer is so thin that the channel needs to be seen from an isometric viewpoint for clarity in figure 9). This is mainly due to the hydrogen thermal conductivity being an order of magnitude smaller than that of the nickel solid. The maximum tip coolant temperature is 703 K.

The solid stresses induced by the thermal gradient are shown in figure 10, and figure 11 depicts the spanwise displacement for the solid model. From figure 10, high compressive stresses are found near the leading edge while maximum tension is situated near the +/-90 degree radius angle of the leading edge. The compressive stress in the ZZ component (across the thickness direction) also corresponds to the expansion in the spanwise displacement as evidenced in figure 11.

To validate the current solution convergence, we have compared, in figures 12 and 13, temperature and velocity profiles along two selected line probes using two different fluid mesh densities. The densities, respectively, are 4323 (referred to as mesh 1 in the figure legend) and 7139 elements (mesh 2). The first line probe (referred to as “centerline” in the figure legend) is located along the centerline of the leading edge region spanning both the solid and coolant channel region (line probe origin at the coolant region). The second one (“60 degree”) cuts along the 60-degree radius line in the leading edge region. The agreement between the two solutions is excellent. Note that the solid region consists of zero velocity and near-linear temperature profiles on the right side of the plots.

Case 2: 2D full coolant, solid, and external flow thermal interactions

The full 2D coolant, solid model and external flow thermal interactions involve solutions of incompressible thermal, solid thermal/stress, and compressible flow equations. To start the FSI computation, a steady-state external flow at Mach 5 with adiabatic wall condition was used as the initial condition. Figures 14 and 15 show the final FSI external Mach number contours in global and local views, respectively. The strong bow shock upstream of the leading edge is resolved clearly. Strong deceleration behind the bow shock forming an external stagnation region is also observed.

The temperature contours is depicted in figures 16 and 17 in both the global and local views. The temperature jump induced by the shock wave is again well resolved. The maximum temperature is about 1800 K located in the external stagnation region. But the maximum temperature on the solid surface has been drastically reduced to 418 K with active cooling. Although the results are not shown here, the aerothermodynamic heating with adiabatic wall condition (without cooling) generated a peak wall temperature about 1807 K. Furthermore, the heat generated at the nose region was convected downstream heating the whole solid surface.

The thermal distributions in the solid model and coolant region are illustrated separately in figures 18 and 19 due to the scale disparity. The maximum tip temperature is 418 K for the solid and 381 K for the coolant. The contour distributions are similar to those of case 1; that is, near linear profile in the solid region and thin “boundary-layer” type profile in the coolant region.

Finally, the temperature profiles at two line probes across the three regions near the leading edge are plotted in figure 20. The locations of the line probe are the same as those of figure 14 (except they extend into the external region now). Meshes 1 and 2 have 8959 and 12905 hexahedral elements, respectively. The two mesh solutions agree with each other reasonably well. From the right, it is

seen clearly that the temperature experiences a sudden increase through the external shock wave, stays relatively constant in the external stagnation region, and then develops an external thermal boundary layer near the nose. The temperature gradient then stays relatively linear inside the solid model region. A very sharp temperature gradient again is observed on the coolant side of the interface.

Case 3: Semi 3D coolant and solid thermal interactions

To demonstrate the effectiveness of different design impingement models, coolant/solid thermal interactions have been simulated on two semi-3D models. It is semi-3D since we assume the internal coolant flow to be two-dimensional while the solid model is fully 3D. Except for the spanwise dimension, the overall geometry is similar to that of Case 1. In addition, these two cases differ mainly in the area of the impingement region. The flow conditions are the same as those of Case 1.

Figures 21 and 22 compare the velocity and temperature contours of the two different configurations. It is seen that different channel configurations produce dramatically different flow patterns in the stagnation region. The top configuration exhibits a significantly larger area of stagnant flow, hence, reducing cooling effectiveness. Both cases have the same inlet flow condition; however, the maximum total velocity in the top configuration is about 300 m/sec, as compared to 412 m/sec for the bottom one. The final maximum solid surface temperature also differs significantly. The top configuration has a maximum tip temperature of 1200 K vs. 800 K for the bottom one. It is demonstrated that the bottom configuration is much more effective as an active cooling design.

Conclusion

The ability of Spectrum to perform multiphysics simulations of an actively cooled hypersonic leading edge has been successfully demonstrated with these results. The cases simulated included 2D and semi-3D coolant/solid thermal interactions under specified heat flux to study the coolant flow physics and the 2D multiphysics aerothermodynamic interactions. It was shown that the leading edge develops significant thermal gradients at steady state. In particular, the coolant and structural thermal gradients are extremely large near the tip/stagnation region of the component. Solution convergence in these problems was demonstrated from mesh refinement analyses.

The cases analyzing coolant, solid, and external Mach 5 hypersonic flow interactions have demonstrated the effectiveness of active cooling. The external aerothermodynamic surface heating due to shock wave and stagnation has been greatly reduced from 1807 K to 418 K. Without cooling, the nickel solid would experience material failure. Finally, we have also illustrated the importance of internal coolant channel design by comparing the flow and thermal physics between two different channel configurations.

References

[1] Melis, M.E., Gladden, H.J., Schubert, J.F., Westfall, L.J. and Trimarchi, P.A., "A Unique Interdisciplinary Research Effort to Support Cowl Lip Technology Development for Hypersonic Applications," NASA Technical Paper 2876, 1989.

[2] Hughes, T.J.R. and Mallet, M., "A New Finite Element Formulation for Computational Fluid Dynamics: III. The Generalized Streamline Operator for Multidimensional Advective-Diffusive Systems," Computer Methods in Applied Mechanics and Engineering, Vol. 58, pp. 305-328, 1986.

[3] Hughes, T.J.R., Franca, L.P., and Balestra, M., "A New Finite Element Formulation for Computational Fluid Dynamics: V. Circumventing the Babuska-Brezzi Condition: A Stable Petrov-Galerkin Formulation of the Stokes Problem Accommodating Equal-order Interpolations," Computer Methods in Applied Mechanics and Engineering, Vol. 59, pp. 85-99, 1986.

[4] Hughes, T.J.R. and Franca, L.P., "A New Finite Element Formulation for Computational Fluid Dynamics: VII. The Stokes Problem with Various Well-Posed Boundary Conditions: Symmetric Formulations that Converge for all Velocity/Pressure Spaces," Computer Methods in Applied Mechanics and Engineering, Vol. 65, pp. 85-96, 1987.

[5] Hughes, T.J.R., Franca, L.P. and Hulbert, G.M., "A New Finite Element Formulation for Computational Fluid Dynamics: VIII. The Galerkin/Least-Squares Method for Advective-Diffusive Equations," Computer Methods in Applied Mechanics and Engineering, Vol. 73, pp. 173-189, 1989.

[6] Franca, L.P. and Hughes, T.J.R., "Convergence Analyses of Galerkin/Least-Squares Methods for Symmetric Advective-Diffusive Forms of the Stokes and Incompressible Navier-Stokes Equations," Computer Methods in Applied Mechanics and Engineering, Vol. 105, pp. 285-298, 1993.

[7] Hauke, G. and Hughes, T.J.R., "A Unified Approach to Compressible and Incompressible Flows," Computer Methods in Applied Mechanics and Engineering, Vol. 113, pp. 389-396, 1994.

[8] Johnson, C, Szepessy, A. and Hansbo, P., "On the Convergence of Shock-Capturing Streamline Diffusion Finite Element Methods for Hyperbolic Conservation Laws," Mathematics of Computation, Vol. 54, pp. 107-129, 1990.

[9] Nomura, T. and Hughes, T.J.R., "An Arbitrary Lagrangian-Eulerian Finite Element Method for Interaction of Fluid and a Rigid Body," Computer Methods in Applied Mechanics and Engineering, Vol. 95, pp. 115-138, 1992.

[10] Hughes, T.J.R., Zimmermann, T., and Liu, W.K., "Lagrangian-Eulerian Finite Element Formulation for Incompressible Viscous Flows," Computer Methods in Applied Mechanics and Engineering, Vol. 29, pp. 329-349, 1981.

[11] Simo, J.C. and Rifai, M.S., "A Class of Mixed Assumed Strain Methods and The Method of Incompatible Modes," International Journal for Numerical Methods in Engineering, Vol. 29, pp. 1595-1638, 1990.

[12] Simo, J.C., Rifai, M.S. and Fox, D.D., "On a Stress Resultant Geometrically Exact Shell Model. Part IV: Variable Thickness Shells with Through-the-Thickness Stretching," Computer Methods in Applied Mechanics and Engineering, Vol. 80, 1990.

[13] Rifai, S.M., Johan, Z., Wang, W.-P., Hughes, T.J.R, and Ferencz, R.M., "Multiphysics simulation of flow-induced vibrations and aeroelasticity on parallel computing platforms," special issues in "Parallel Computational Methods for Flow Simulation and Modeling", Computer Methods in Applied Mechanics and Engineering, 1999 (to appear).

[14] Grisval, J.-P., Sauvignet, C. and Johan, Z., "Aeroelasticity calculations using a finite element method," International Forum on Aeroelasticity and Structural Dynamic, Rome, Italy, June 17-20, 1997.

[15] Gielda, T.P., Webster, B.E., Hesse, M.E., and Halt, D.W., "The Impact of Computational Fluid Dynamics on Automotive Interior Comfort Engineering," AIAA Paper 96-0794, 34th Aerospace Sciences Meeting and Exhibit, January 1996.

[16] Rifai, S.M., Ferencz, R., Wang, W.-P., Spyropoulos, E., Lawrence, C., and Melis, M., "The role of multiphysics simulation in multidisciplinary analysis," AIAA 98-4863, 1998.

[17] Wang, W.-P., Rifai, S.M., and Hughes, T.J.R., “Multiphysics Simulations of Aeropropulsion Systems Using Smart Structures,” AIAA99-0368, 1999.

[18] Killackey, J.J., Katinszky, E.A., Tepper, S., Vuigner, A.A, Wright, C.C., and Stockwell, G.G., “Thermal-Structural Design Study of an Airframe Integrated Scramjet. Final Report, June 1975-Dec. 1979,” NASA CR-159039, 1980.

[19] Incropera, F.P. and DeWitt, D.P., “Fundamentals of Heat and Mass Transfer,” John Wiley, 2nd ed., 1985.

[20] Centric Engineering Systems, Spectrum Theory Manual, Santa Clara, CA, 1993.

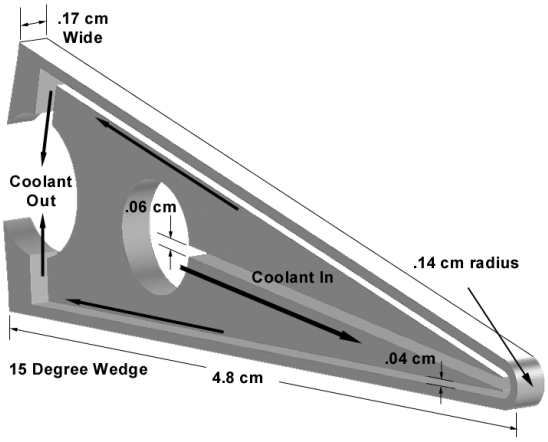

Figure 2. Schematic of the leading edge model.

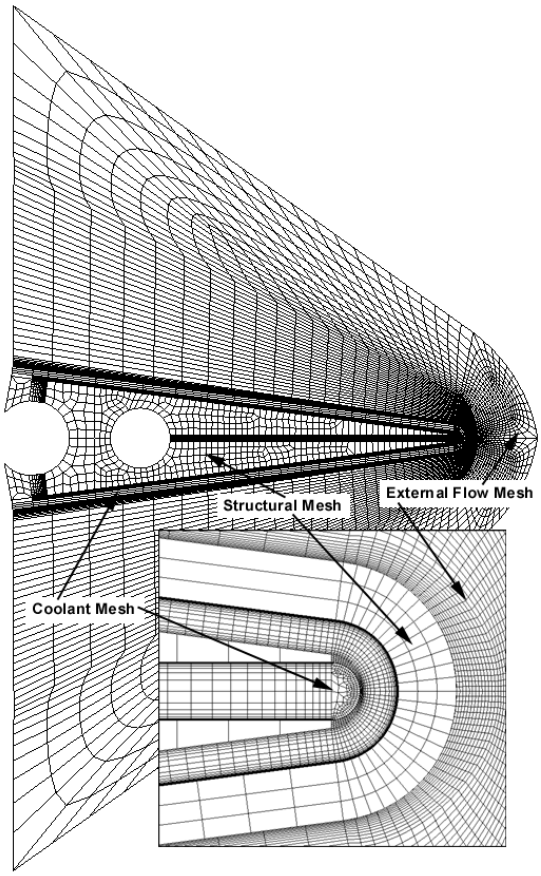

Figure 3. Mesh showing all three regions: coolant channel, solid model, and external flow.

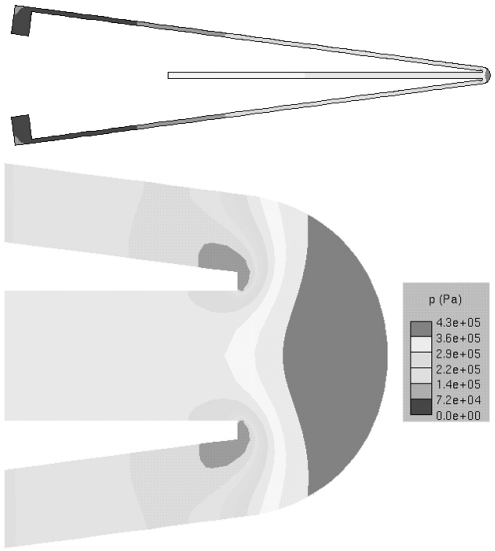

Figure 4. Coolant pressure contours in global and local views; Case 1

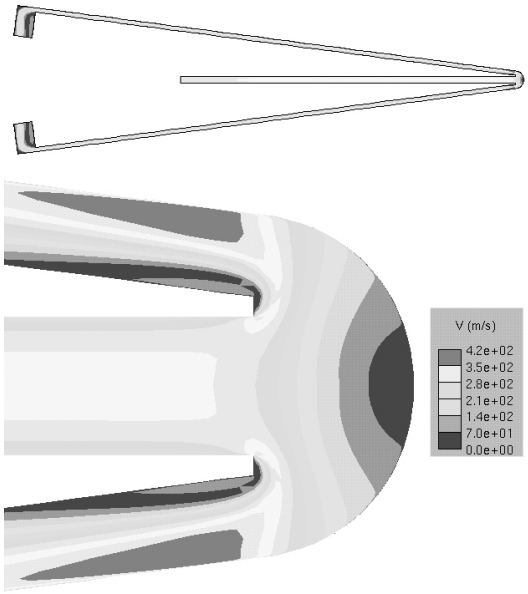

Figure 5. Coolant velocity contours in global and local views; Case 1

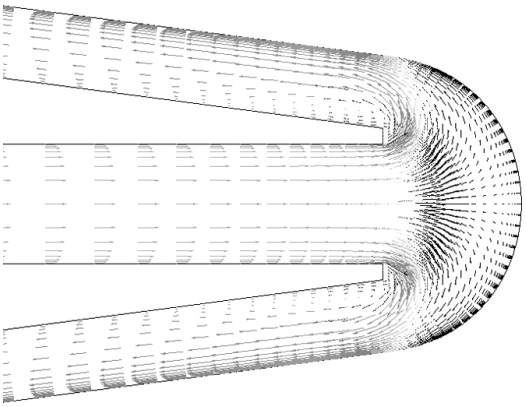

Figure 6. Coolant velcoity vectors near leading edge; Case 1

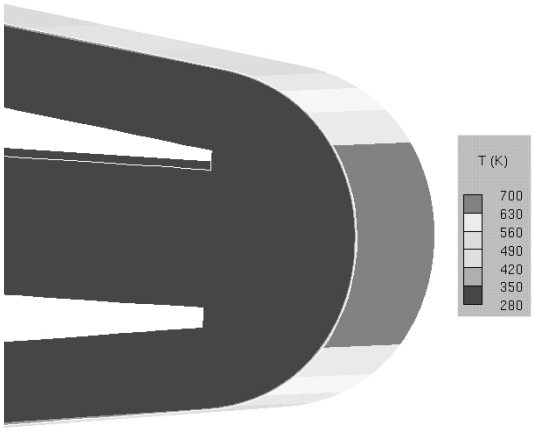

Figure 9. Coolant temperature contours under specified heat flux; Case 1

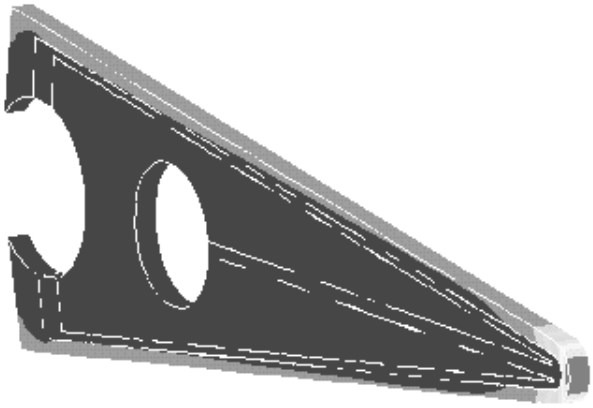

Figure 7. Solid Surface temperature under specified heat flux; Case 1

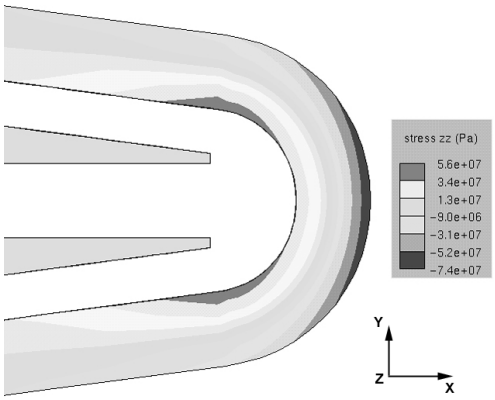

Figure 10. ZZ solid stress contours under specified heat flux; Case 1

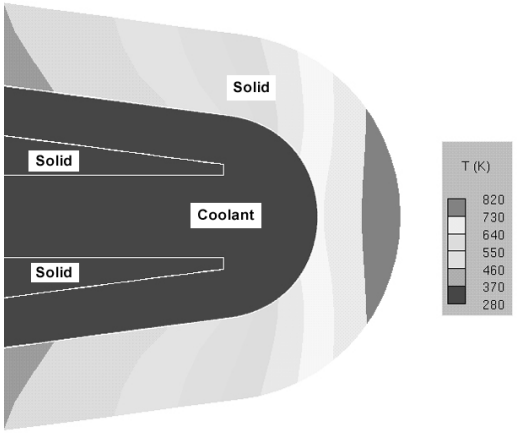

Figure 8. Solid model temperature distribution under specified heat flux; Case 1

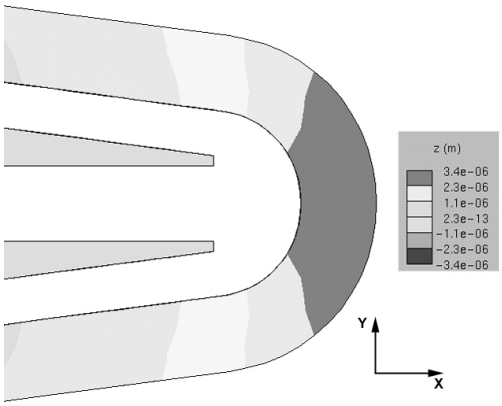

Figure 11. Spanwise displacement for the solid model under specified heat flux; Case 1

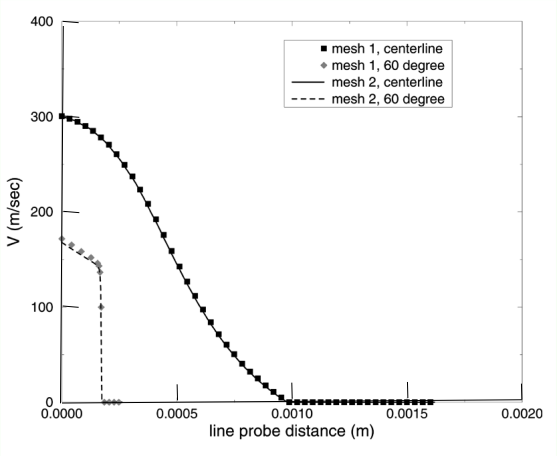

Figure 12. Comparison of velocity profile at two different line probes for two different meshes; Case 1

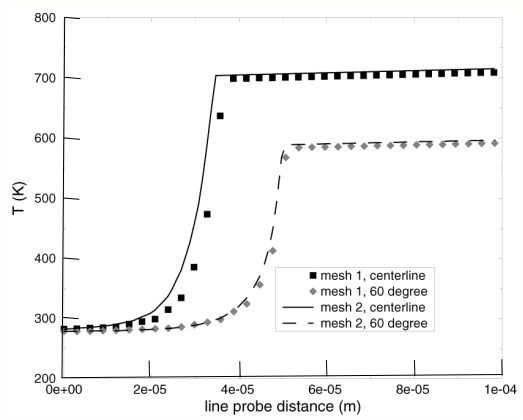

Figure 13. Comparison of temperature profiles at two different line probes for two different meshes; Case 1

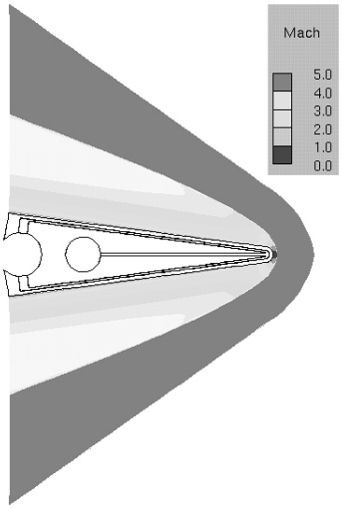

Figure 14. External flow Mach number contours (legend shown in next figure); Case 2

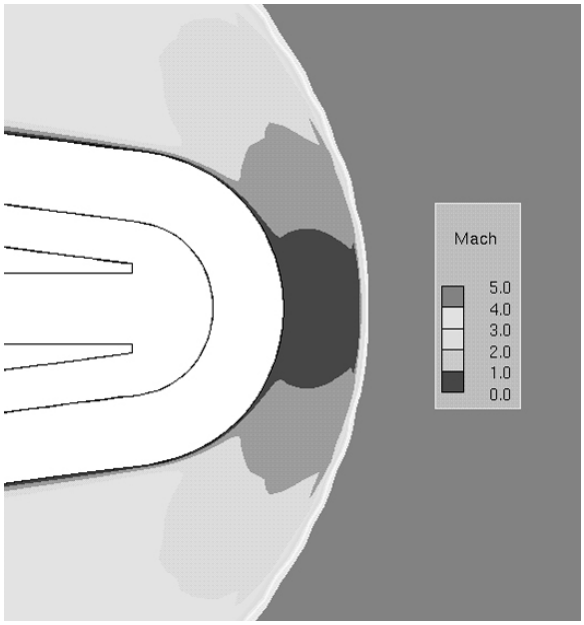

Figure 15. Local external flow Mach number contours; Case 2

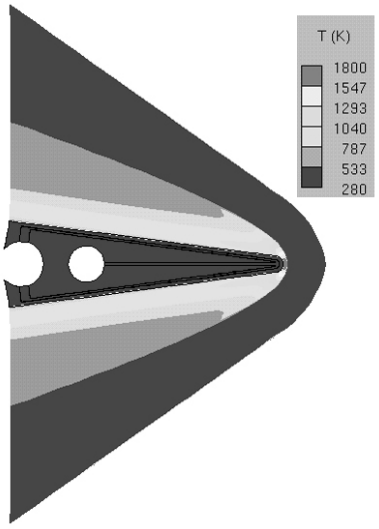

Figure 16. Temperature contours in external flow; global view, Case 2

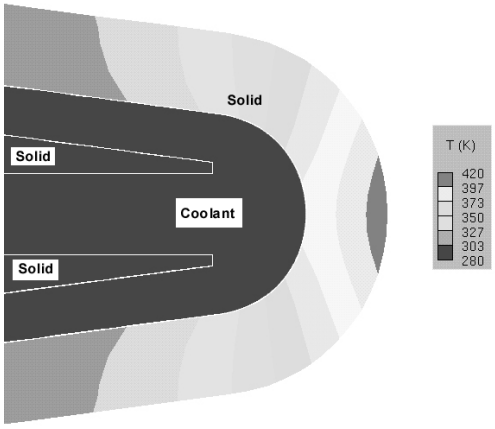

Figure 18. Thermal distribution under active cooling; Solid model only, Case 2

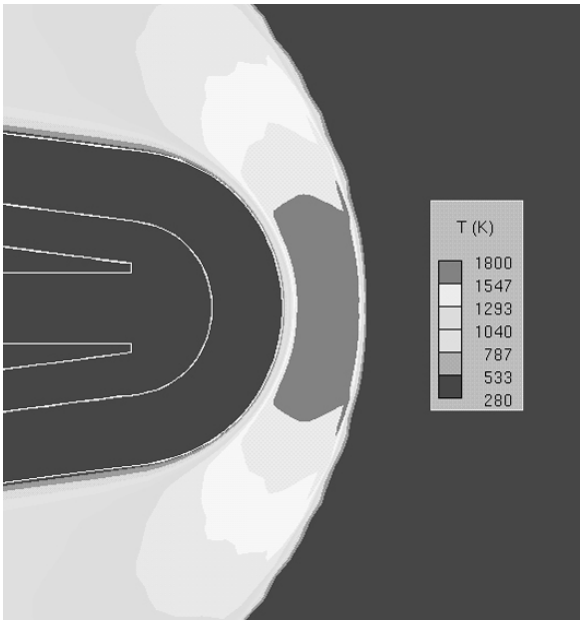

Figure 17. Thermal distribution under active cooling; Case 2

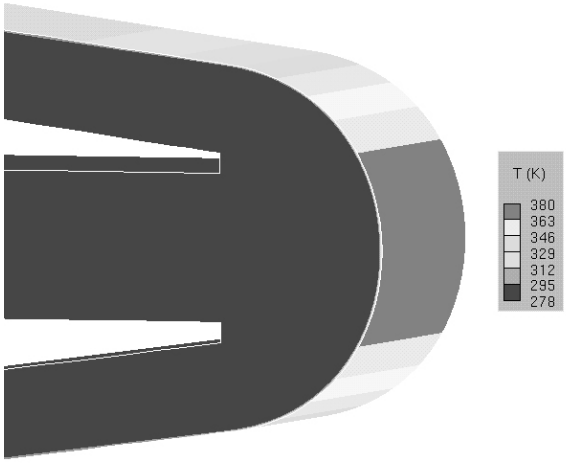

Figure 19. Thermal distribution under active cooling; Coolant channel only, Case 2

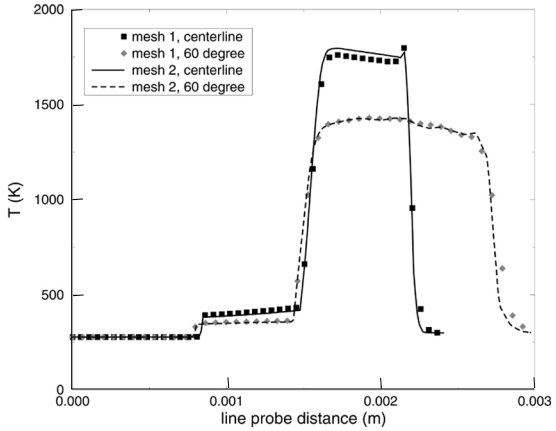

Figure 20. Comparison of temperature profiles at two different line probes for two different meshes; Case 2

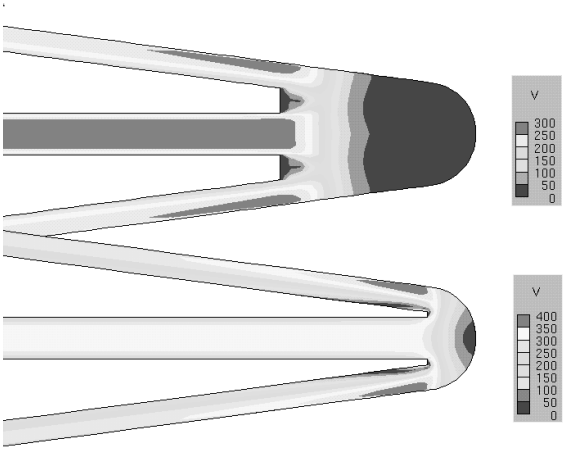

Figure 21. Comparison of velocity contours for two different channel configurations; Case 3

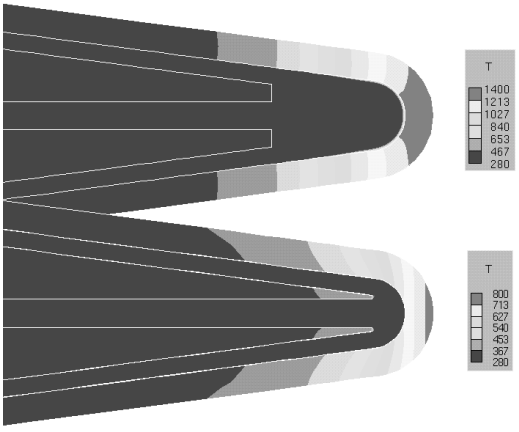

Figure 22. Comparison of temperature contours for two different channel configurations; Case 3

REPORT DOCUMENTATION PAGE

Form Approved
OMB No. 0704-0188

1. AGENCY USE ONLY (*Leave blank*)	2. REPORT DATE	3. REPORT TYPE AND DATES COVERED
	October 1999	Technical Memorandum

4. TITLE AND SUBTITLE

Multiphysics Simulation of Active Hypersonic Cowl Lip Cooling

5. FUNDING NUMBERS

WU–523–61–13–00

6. AUTHOR(S)

Matthew E. Melis and Wen-Ping Wang

7. PERFORMING ORGANIZATION NAME(S) AND ADDRESS(ES)

National Aeronautics and Space Administration
John H. Glenn Research Center at Lewis Field
Cleveland, Ohio 44135–3191

8. PERFORMING ORGANIZATION REPORT NUMBER

E–11731

9. SPONSORING/MONITORING AGENCY NAME(S) AND ADDRESS(ES)

National Aeronautics and Space Administration
Washington, DC 20546–0001

10. SPONSORING/MONITORING AGENCY REPORT NUMBER

NASA TM—1999-209275
AIAA–99–3510

11. SUPPLEMENTARY NOTES

Prepared for the 1999 Norfolk Summer Conference sponsored by the American Institute of Aeronautics and Astronautics, Norfolk, Virginia, June 28—July 1, 1999. Matthew E. Melis, NASA Glenn Research Center, and Wen-Ping Wang, Centric Engineering Systems, 624 E. Evelyn Ave., Sunnyvale, California 94086 (work funded under NASA Contract NAS3–98068). Responsible person, Matthew E. Melis, organization code 5930, (216) 433–3322.

12a. DISTRIBUTION/AVAILABILITY STATEMENT

Unclassified - Unlimited
Subject Categories: 39 and 34 Distribution: Nonstandard

This publication is available from the NASA Center for AeroSpace Information, (301) 621–0390.

12b. DISTRIBUTION CODE

13. ABSTRACT ***(Maximum 200 words)***

This article describes the application of the Multidisciplinary Analysis (MDA) solver, Spectrum ™, in analyzing a hydrogen-cooled hypersonic cowl leading-edge structure. Spectrum, a multiphysics simulation code based on the finite element method, addresses compressible and incompressible fluid flow, structural, and thermal modeling, as well as the interactions between these disciplines. Fluid-solid-thermal interactions in a hydrogen impingement-cooled leading edge are predicted using Spectrum. Two- and semi-three-dimensional models are considered for a leading edge impingement cooling concept under either specified external heat flux or aerothermodynamic heating from a Mach 5 external flow interaction. The solution accuracy is demonstrated from mesh refinement analysis. With active cooling, the leading edge surface temperature is drastically reduced from 1807 K of the adiabatic condition to 418 K. The internal coolant temperature profile exhibits a sharp gradient near channel/solid interface. Results from two different cooling channel configurations are also presented to illustrate the different behavior of alternative active cooling schemes.

14. SUBJECT TERMS	15. NUMBER OF PAGES
Finite element method; Fluid mechanics; Heat transfer; Leading edges; Cryogenic coding	17
	16. PRICE CODE: A03

17. SECURITY CLASSIFICATION OF REPORT	18. SECURITY CLASSIFICATION OF THIS PAGE	19. SECURITY CLASSIFICATION OF ABSTRACT	20. LIMITATION OF ABSTRACT
Unclassified	Unclassified	Unclassified	